

## REDUCTION OF LEAKAGE MAGNETIC FIELD IN ELECTROMAGNETIC SYSTEMS BASED ON ACTIVE SHIELDING CONCEPT VERIFIED BY EIGENVALUE ANALYSIS

F. Faghihi and H. Heydari

Center of Excellence for Power System Automation and Operation  
Electrical Engineering Department  
Iran University of Science and Technology  
Tehran, Iran

**Abstract**—Leakage fields are one of the main issues in design of electromagnetic systems. Some of these fields close their paths through the core and air, giving rise to non-ideal behavior of the magnetic systems. This paper explains a novel concept of active shielding which consists of two compensation coils in series and generates a counter field opposite to the leakage fields leaking from an iron-core system. As the method is based on physical reasoning of electromagnetic coupled circuit theory, the design criterions for the compensating coils parameters, their number of turns and their adaptation to the systems, were considered. The state of the art is presented by a model which is verified by roots of system characteristic equations, using state equations. In a case study, this method was investigated in a 25 kA (125 kVA) current injection transformer (CIT) system delivering a secondary current as closely proportioned to the primary current as possible, using finite element method (FEM) simulation.

This paper will also push the state of the art by reducing the age effect of the CIT through mechanical force reduction.

### 1. INTRODUCTION

Leakage magnetic fields contribute to several undesirable effects in many applications [1,2]. As a consequence, there is considerable interest in reducing such fields [3,4]. This paper presents a novel concept for minimizing leakage fields by generating a field that opposes the leakage field.

---

Corresponding author: H. Heydari (heydari@iust.ac.ir).

However, there is a likelihood of confusion by considering issues of arguable fact on leakage field and stray field. It is important to make a very clear distinction between leakage field and stray field. The leakage is formed by the flux that links one winding and does not link the other winding. It can be measured as a voltage drop at the transformer terminals. The leakage flux does not necessarily escape the transformer. Stray fields necessarily escape the transformer. The stray flux can link one or two of the windings. Stray flux can exist in the air without adding to the leakage inductance. The stray flux is not measured as a voltage drop at the terminals. It can be measured with a coil in the neighborhood of the transformer. A portion of the leakage flux can also be stray flux when it escapes the transformer boundaries. Stray fields occasionally bring about disturbing electromagnetic environment which may lead to electromagnetic interferences (EMI) with other neighbouring sensitive components/systems. The standard solution to the problem of stray fields is the addition of passive shielding (metal enclosure) with shielding high effectiveness. This solution is effective although frequently is not economical. On the other hand, the effective solution to leakage flux is active shielding, which is the main motivation for initiating this paper [5].

The strategy proposed in this paper is based on active shielding that is, to producing an opposite magnetic field by two compensating windings. The method of inter-connecting the two windings and their resistance values are important issue and hence discussed in this paper. Using basic electromagnetic laws, the physical reasoning and mathematical models of coupled circuits based on state equations are presented. A case study for analysis of improvement of electromagnetic system (i.e., any machines having magnetic core and windings) stability speed using characteristic roots is included.

## **2. ANALYSIS OF LEAKAGE MAGNETIC FIELDS IN ELECTROMAGNETIC SYSTEMS**

Since a transformer is the simplest and the most applicable electromagnetic system the leakage fields, in this system, would cause nonlinear relation between current and field consequently leading to incompatibility in induced voltage/current levels with respect to the proportion as the number of turns in the secondary and primary coils, thereby lowering the performance of the system. Fig. 1 shows the FEM simulated leakage and linkage flux distribution in a typical transformer [4] as a starting point for the analysis. In this figure, the leakage flux and the main flux (linkage flux) are shown.

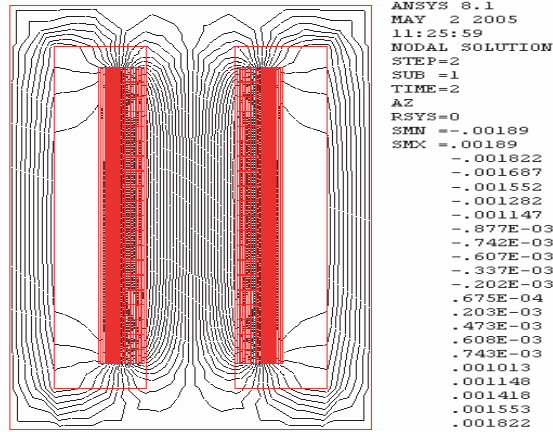


Figure 1. Main and leakage fluxes in a transformer [4].

As mentioned earlier, in an electromagnetic system, the leakage field closes its route outside the core. As a consequence, a transformer having a core with primary and secondary windings, the applied voltage  $v_1$  pushes current  $i_1$  in the primary winding from which total primary field  $\widehat{\varphi}_1$  is produced. This field comprises of two components  $\varphi_{m_1}$  and  $\varphi_{l_1}$ , encompassing the whole primary winding turns:

$$\widehat{\varphi}_1 = \varphi_{m_1} + \varphi_{l_1} \tag{1}$$

where,  $\varphi_{m_1}$  is mutual field between primary and secondary windings being created by  $i_1$ , and  $\varphi_{l_1}$  is primary leakage field being only linked with primary windings.  $\varphi_{l_1}$  has two components:

$$\varphi_{l_1} = \varphi_{11} + \varphi_{12} \tag{2}$$

where,  $\varphi_{11}$  is self leakage field of the primary winding and  $\varphi_{12}$  is leakage field due to secondary winding encompasses primary winding.

Since  $\varphi_{m_1}$  varies with time, so an emf is induced in the secondary winding, so that if its ends are connected so as to complete the circuit a current  $i_2$  will flow in the secondary coil producing field  $\varphi_{m_2}$  having a direction tends to counterbalance the original change in field  $\varphi_{m_1}$  (Lenz’s law). In another word, the current  $i_2$  in secondary winding creates a total field  $\widehat{\varphi}_2$  linking all the secondary winding comprises of two components:

$$\widehat{\varphi}_2 = \varphi_{m_2} + \varphi_{l_2} \tag{3}$$

However,  $\varphi_{m_2}$  mutual inductance due to  $i_2$  links both primary and secondary windings and secondary leakage field  $\varphi_{l_2}$  only linking

secondary winding comprises of two components  $\varphi_{22}$  and  $\varphi_{21}$ :

$$\varphi_{l_2} = \varphi_{22} + \varphi_{21} \quad (4)$$

where,  $\varphi_{22}$  is self leakage field of the secondary winding and  $\varphi_{21}$  is leakage field due to primary winding links secondary winding. Now the simultaneous current flow of  $i_1$  and  $i_2$  gives rise to creation of two main fields  $\varphi_{m_1}$  and  $\varphi_{m_2}$  from which the resultant field  $\varphi$  encompasses both windings:

$$\varphi = \varphi_{m_1} - \varphi_{m_2} \quad (5)$$

Now, by considering total fields  $\varphi_1$  and  $\varphi_2$ , total field linkage  $\psi_1$  and  $\psi_2$  encompassing both primary and secondary windings, the analytical equations of leakage field are as follow:

$$\varphi_1 = \varphi + \varphi_{l_1} \quad (6)$$

$$\varphi_2 = \varphi + \varphi_{l_2} \quad (7)$$

$$\psi_1 = N_1\varphi_1 = N_1(\varphi + \varphi_{11} + \varphi_{12}) \quad (8)$$

$$\psi_2 = N_2\varphi_2 = N_2(\varphi + \varphi_{21} + \varphi_{22}) \quad (9)$$

Applying KVL, gives rise to the following voltage equations:

$$v_1 = R_1 i_1 + \frac{d\psi_1}{dt} \quad (10)$$

$$v_2 = R_2 i_2 + \frac{d\psi_2}{dt} \quad (11)$$

where,  $R_1$  and  $R_2$  are the effective resistances of primary and secondary windings respectively.

To achieve such a case the leakage field must be weakened to the maximum extent, so that the voltage/current ratio is as closely proportioned to the turn ratio as possible.

### 3. DESIGN PARAMETERS BASED ON ACTIVE SHIELDING CONCEPT

An important component of the losses generated in the magnetic systems is due to leakage fields leaking from their magnetic core and they may penetrate into electrically conducting construction parts, mostly made of solid, unlaminated steel, in which eddy currents are generated. Such leakage fields induced losses partially located in different parts of the system.

However, shielding of the leakage field can reduce losses if it is done appropriately. In any electromagnetic system, compensation of leakage fields is based on two methods: Active and passive shielding [5–8]. In order to mitigate undesired effects of leakage fields penetration

into the main system, in the passive shielding method one uses a high permeability magnetic material and shields by a mechanism called “field shunting”: The field from a source is diverted into a magnetic material and away from the region to be shielded [8, 9].

The normal passive shielding technique is not always convenient to mitigate the extremely low frequency (ELF) magnetic fields [7–9]. In some practical applications since a large quantity of material can be often required to build a shield adequate to mitigate low frequency magnetic fields, even more important than required materials, the nature of the electromagnetic system causes this method useless. Leakage fields are coupled with the magnetic system, therefore for the purpose of the subject under discussion, this method is useless.

In the course of leakage field mitigation, a better solution is to design a system of low frequency compensating current coils that is, *active shielding* producing fields as oppose to the disturbing fields. In the active shielding method one tries to attenuate all the sources of frequencies below a certain limiting value determined by the control system consisting of compensating coils producing fields of opposite phases.

The purpose of this paper is to reduce the leakage field based on new field source with maximum possible neutralization capability without having any disturbances to inter-connected systems or peripheral devices [5]. However, the new source is designed by two compensating coils being wound on the same core as for the primary and secondary coils. The crucial point is that all four coils are source of field generation and therefore induced voltages on the compensating coils are unavoidable. Since these compensating coils are liable to leakage and mutual fields therefore, their polarities are crucial to oppose the leakage fields generated by  $N_1$  and  $N_2$ , to keep the system close to the ideal state.

However, the compensating coils are neither directly excited by a source nor connected to any device, so they are inter-connected with each other through a resistor (if it is necessary) or directly. It is interesting to note that the current flowing in the closed loop of the active shielding coils is due to Lenz law phenomenon from which the outcome fields are to counterbalance the leakage fields of the main coils. This theory was verified by wrapping the right order of the coils  $N_3$ ,  $N_1$ ,  $N_2$  and  $N_4$  round a common limb of the core, respectively, as shown in Fig. 2. This configuration can more or less separate the field source by producing positive and negative poles in each pair of main and compensating windings resulted in leakage field reduction. The independency of the main field was obtained by taking the equal number of turns in both compensating coils and also their

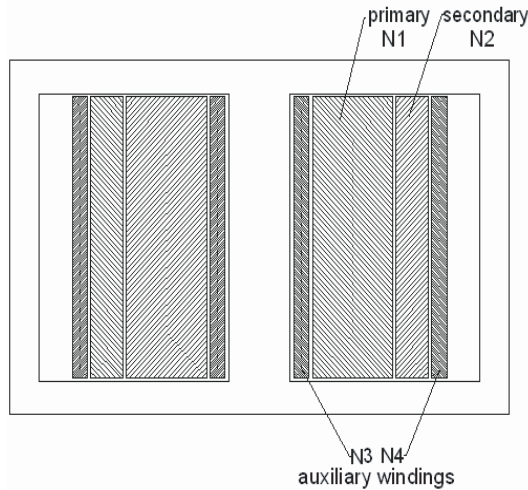


**Figure 2.** Simplified layout of new design configuration with the compensating coils.

inter-connection in parallel form so that connecting like poles together. This ensures that zero induced voltage, i.e., no flux linkage, in the compensating coil loop does exist. This implies that the current in the loop ( $i_{aux}$ ) is totally independent of the induced voltages and it is only a function of leakage fields between those of the primary and secondary coils and compensating ones. As such, this current produces a magnetic field to reduce the leakage fields of the two main primary and secondary windings.

#### 4. MATHEMATICAL PRINCIPLES BEYOND THE CONCEPT

This section describes the operating principle of a transformer fitted with two compensating windings, starting from the mathematical model of a four winding transformer core, and considering the classic theory of electromagnetic coupled circuits.

##### 4.1. Basic Principles of the Four Winding Transformer Core

Let us consider Fig. 3 as a schematic model of a transformer with four windings, having positive currents entering their positive terminals, producing fields with the same direction. By ignoring the distributed

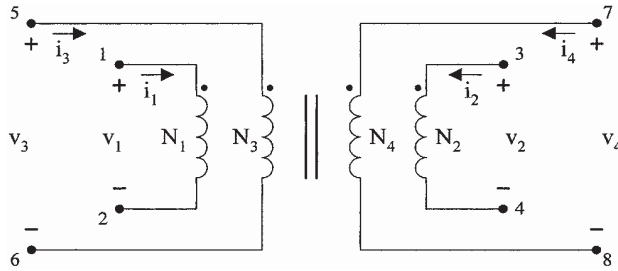


**Figure 3.** Schematic of the mathematical model of a transformer with four windings.

capacitances of the windings, applying Faraday’s law, yields:

$$v_j = R_j i_j + \frac{d\psi_j}{dt} = R_j i_j - e_j \tag{12}$$

where, the subscript  $j$  refers to the index of the winding,  $v$  is the instantaneous terminal voltage,  $i$  is the instantaneous current,  $R$  is the effective resistance,  $\psi$  is the instantaneous field linkage and  $e$  is the instantaneous voltage induced by the time-varying field linkages.

Suppose the permeability of the core is constant (no saturation), the field linkages are proportional to the currents producing them and consequently, on the basis of superposition, the field linkages can be expressed as the sum of the components produced by each current acting alone. To simplify the study of the magnetic field in the transformer, let us introduced the concept of field  $\phi_j$ , as the per turn average field linkage with winding  $j$

$$\phi_j = \frac{\psi_j}{N_j} \tag{13}$$

The average field linkage with each winding can be divided into three main components.

- 1) The resultant flux,  $\phi$  linking all the windings, produced by the combination of currents  $i_1, i_2, i_3$  and  $i_4$ . Considering the resultant field exclusively confined to the core.
- 2) The winding self-flux,  $\phi_{jj}$  being produced by its individual current,  $i_j$  accounting for the leakage field of each winding, with four components:
  - a) The flux linking only each individual winding;
  - b) The flux linking the individual winding and second winding;
  - c) The flux linking the individual winding and third winding;
  - d) The flux linking the individual winding and fourth winding.

- 3) The mutual flux between pairs of coils,  $\phi_{jk}$  which accounts for the field produced by current linking only winding  $N_j$ .

Therefore, the field linkage with each winding is written as:

$$\psi_1 = N_1 (\phi + \phi_{11} + \phi_{12} + \phi_{13} + \phi_{14}) \quad (14)$$

$$\psi_2 = N_2 (\phi + \phi_{21} + \phi_{22} + \phi_{23} + \phi_{24}) \quad (15)$$

$$\psi_3 = N_3 (\phi + \phi_{31} + \phi_{32} + \phi_{33} + \phi_{34}) \quad (16)$$

$$\psi_4 = N_4 (\phi + \phi_{41} + \phi_{42} + \phi_{43} + \phi_{44}) \quad (17)$$

where,  $N_1$ ,  $N_2$ ,  $N_3$  and  $N_4$  are primary, secondary, and two adapted compensating windings, respectively. Since the self and mutual flux components entirely or partially close their paths in air, and it is well known that the reluctance of air path is very high compared to that of the magnetic core; in this case we can introduce the self-inductance  $l_{jj}$  and the mutual inductance  $l_{jk}$  coefficients  $j, k \in \{1, 2, 3, 4\}$ . Thus, Equations (14) through (17) becomes

$$\psi_1 = N_1\phi + l_{11}i_1 + l_{12}i_2 + l_{13}i_3 + l_{14}i_4 \quad (18)$$

$$\psi_2 = N_2\phi + l_{21}i_1 + l_{22}i_2 + l_{23}i_3 + l_{24}i_4 \quad (19)$$

$$\psi_3 = N_3\phi + l_{31}i_1 + l_{32}i_2 + l_{33}i_3 + l_{34}i_4 \quad (20)$$

$$\psi_4 = N_4\phi + l_{41}i_1 + l_{42}i_2 + l_{43}i_3 + l_{44}i_4 \quad (21)$$

Substituting the flux linkage of each individual winding from Equations (18) through (21) in Equation (12), their corresponding instantaneous terminal voltages can be obtained, respectively:

$$v_1 = R_1i_1 + N_1 \frac{d\phi}{dt} + l_{11} \frac{di_1}{dt} + l_{12} \frac{di_2}{dt} + l_{13} \frac{di_3}{dt} + l_{14} \frac{di_4}{dt} \quad (22)$$

$$v_2 = R_2i_2 + N_2 \frac{d\phi}{dt} + l_{21} \frac{di_1}{dt} + l_{22} \frac{di_2}{dt} + l_{23} \frac{di_3}{dt} + l_{24} \frac{di_4}{dt} \quad (23)$$

$$v_3 = R_3i_3 + N_3 \frac{d\phi}{dt} + l_{31} \frac{di_1}{dt} + l_{32} \frac{di_2}{dt} + l_{33} \frac{di_3}{dt} + l_{34} \frac{di_4}{dt} \quad (24)$$

$$v_4 = R_4i_4 + N_4 \frac{d\phi}{dt} + l_{41} \frac{di_1}{dt} + l_{42} \frac{di_2}{dt} + l_{43} \frac{di_3}{dt} + l_{44} \frac{di_4}{dt} \quad (25)$$

Considering Equations (22) through (25), the corresponding instantaneous terminal voltage of each winding, ( $v_1$ ,  $v_2$ ,  $v_3$  and  $v_4$ ) is the sum of the winding resistance voltage drop, the emf due to the time varying resultant flux, and induced electromotive forces associated with the self and mutual leakage fluxes. The inductive elements in (22) to (25) can be represented in a  $4 \times 4L - M$  matrix containing only leakage inductances with ten independent elements, four diagonal ( $l_{jj}$ ) and six off diagonal ( $l_{jk} = l_{kj}$ ).

### 4.2. Mathematical Analysis for the Offered Configuration

Let us consider the transformer supplying power to a load and the compensating coils connected as shown in Fig. 4. In relation to Fig. 3, now  $i_2 = -i_o$  where  $i_o$  is the load current.

As stated before,  $N_3$  and  $N_4$  are inter-connected parallel (terminals 5 and 6 are connected to terminals 7 and 8, respectively), so that to work as subtractive mode. This circuit exemplifies the normal operating condition of the transformer. Considering Fig. 4 that  $i_4 = -i_3 = i_{aux}$  and applying this into all Equations (22) through (25) and taking into consideration that  $N_3 = N_4 = N_{aux}$ , yields, respectively:

$$v_1 = R_1 i_1 + N_1 \frac{d\phi}{dt} + l_{11} \frac{di_1}{dt} - l_{12} \frac{di_o}{dt} + (l_{14} - l_{13}) \frac{di_{aux}}{dt} \quad (26)$$

$$v_2 = R_2 i_o + N_2 \frac{d\phi}{dt} + l_{21} \frac{di_1}{dt} - l_{22} \frac{di_o}{dt} + (l_{24} - l_{23}) \frac{di_{aux}}{dt} \quad (27)$$

$$v_3 = -R_3 i_{aux} + N_{aux} \frac{d\phi}{dt} + l_{31} \frac{di_1}{dt} - l_{32} \frac{di_o}{dt} + (l_{34} - l_{33}) \frac{di_{aux}}{dt} \quad (28)$$

$$v_4 = R_4 i_{aux} + N_{aux} \frac{d\phi}{dt} + l_{41} \frac{di_1}{dt} - l_{42} \frac{di_o}{dt} + (l_{44} - l_{43}) \frac{di_{aux}}{dt} \quad (29)$$

It should be noted that we connect  $N_3$  and  $N_4$  through a resistor  $R_a$  (Fig. 4), therefore  $v_4 = v_3 + R_a i_{aux}$ , which yields:

$$\begin{aligned} & (l_{31} - l_{41}) \frac{di_1}{dt} + (l_{42} - l_{32}) \frac{di_o}{dt} \\ & = (R_{aux} - R_a) i_{aux} + l_{aux} \frac{di_{aux}}{dt} - M_{aux} \frac{di_{aux}}{dt} \end{aligned} \quad (30)$$

where,  $R_{aux} = R_3 + R_4$ ,  $l_{aux} = l_{33} + l_{44}$  and  $M_{aux} = l_{34} + l_{43}$ .

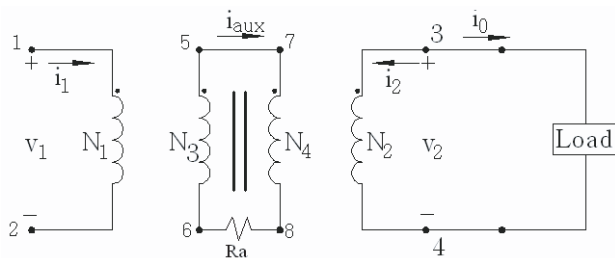


**Figure 4.** New windings configuration of the transformer to counterbalance the leakage fields.

### 4.3. Analytical Study of the Proposed Design Criterion

The current passing through the compensating coils is governed by Equation (30). It is interesting to note that  $i_{\text{aux}}$  is independent of the time derivative of the resultant flux,  $\phi$ . As  $N_3 = N_4$  then  $i_{\text{aux}}$  is a consequence of the coupling leakage flux sharing between  $N_1$  and  $N_2$  leakage flux encompassing  $N_3$  and  $N_4$ . Moreover,  $i_{\text{aux}}$  results from the difference between the leakage mutual inductance coefficients of  $N_1$  and  $N_2$  with respect to  $N_3$  and  $N_4$ , multiply by the time derivative of the primary and secondary currents. On the other hand,  $i_{\text{aux}}$  produces a flux opposing the primary and secondary leakage flux. In order to provide a condition that the current,  $i_{\text{aux}}$  passes across the compensating windings,  $N_3$  and  $N_4$ , during variation of the primary and secondary current,  $i_1$  and  $i_2$  respectively, four cases were concluded using Equation (30), consider an analysis of Fig. 4:

- 1)  $di_o/dt \neq 0$  and  $di_1/dt \neq 0$  but  $i_{\text{aux}} = 0$ , i.e.,  $(l_{31} - l_{41}) = 0$  and  $(l_{42} - l_{32}) = 0$ . This condition is achieved when  $N_3$  and  $N_4$  are positioned on the core so that the primary and secondary leakage fluxes completely encompass them.
- 2)  $di_o/dt = 0$  and  $di_1/dt \neq 0$ ,  $i_{\text{aux}} \neq 0$ . This condition is achieved when  $i_{\text{aux}}$  produces a flux in opposite to the primary leakage flux.
- 3)  $di_o/dt \neq 0$  and  $di_1/dt = 0$ ,  $i_{\text{aux}} \neq 0$ . This condition is achieved when  $i_{\text{aux}}$  produces a flux in opposite to the secondary leakage flux.
- 4)  $di_o/dt \neq 0$  and  $di_1/dt \neq 0$ ,  $i_{\text{aux}} \neq 0$ . This condition is achieved when  $i_{\text{aux}}$  produces a flux that in opposite to both the primary and secondary leakage fluxes.

However, we can say that the compensating current,  $i_{\text{aux}}$  is a function of the leakage flux coupling of the primary and secondary with the third and fourth windings, which generates a magnetic flux opposing the leakage flux of the primary and secondary windings. Consequently, the leakage inductance in the transformer is reduced. The beauty of the fact is that the resultant of the main flux  $\phi$  is not affected by the compensating windings at all.

To optimize the operation of the compensating windings the current  $i_{\text{aux}}$  should be maximized, in order to reduce the leakage inductance of the transformer. This should be noted in transformer design parameters. Nevertheless, there is always some leakage flux escape from primary and secondary that does not link with the compensating windings, even the compensating windings are linked to all the leakage flux in the transformer. However, for minimum leakage flux, there should be a balance between the leakage flux and the current produced by the compensating windings. Referring to (30), the

best way to optimize the operation of the compensating windings is to assemble the transformer in such a way that one compensating winding is preferentially coupled with the primary and the other is preferentially coupled with the secondary. For example, due to the geometric position of the four windings in the transformer, if we consider that the primary leakage flux linked preferentially with the third winding and the secondary leakage flux linked preferentially with the fourth winding, then  $l_{31} \gg l_{41}$  and  $l_{42} \gg l_{32}$ . These are mathematical analyses which are in quite agreement with the arrangement shown in Fig. 2.

Furthermore, Equation (30) can be rewritten as linear first order ordinary differential equation:

$$\begin{aligned} & \frac{di_{\text{aux}}}{dt} + \frac{(R_{\text{aux}} - R_a)}{(l_{\text{aux}} - M_{\text{aux}})} i_{\text{aux}} \\ &= \frac{(l_{31} - l_{41})}{(l_{\text{aux}} - M_{\text{aux}})} \frac{di_1}{dt} + \frac{(l_{42} - l_{32})}{(l_{\text{aux}} - M_{\text{aux}})} \frac{di_o}{dt} = B(t) \end{aligned} \quad (31)$$

And the time constant is given by:

$$\tau = \frac{(l_{\text{aux}} - M_{\text{aux}})}{(R_{\text{aux}} - R_a)} \quad (32)$$

Referring to Equation (32), in order to achieve fast convergence (i.e., rise time reduction) therefore,  $\tau$  must be minimum. This implies that, the denominator of Equation (32) must be maximal that is, the only controllable parameter,  $R_a$  must be zero. This factor has been verified by the case study in Section 5.2.

However, optimal performance of active shielding is commensurate with increase in number of turns of corresponding windings ( $N_3$  and  $N_4$ ). However, the remaining trade-off involves selecting the appropriate number of turns and ohmic losses.

#### 4.4. Verification of the Presented Model Using State Equations

With the well known methodology of solving a boundary value problem, the determination of the leakage magnetic fields in an electromagnetic system is possible. Taking into account all the Equations (26), (27) and (30) the obtained results show the leakage fields are reduced. This is achieved by converting the physical model into differential equations in the form of state equations ( $\dot{X} = AX + BU$ ,  $Y = CX$ ). Roots of characteristics equation of the system is obtained through Laplace transform using  $|sI - A| = 0$  [10, 11]. It is well known that, the rise time analysis of the system depends on the

vicinity of negative pole positions to the origin, that is the more vicinity to the origin the faster stability of equation variables (i.e., voltage and current) are achieved [12]. In this case higher reduction of the leakage fields in the system occurs. Now, we select the state variables as follow:

$$\begin{aligned}x_1 &= i_1, \\x_2 &= i_o, \\ \bullet \\x_2 &= x_3, \\i_{\text{aux}} &= x_4,\end{aligned}\tag{33}$$

which the magnetic flux in the Equations (26) through (29) substitute with:

$$\varphi = L_{1m} \left[ \left( \frac{1}{N_1} \right) i_1 + \left( \frac{N_2}{N_1^2} \right) i_2 + \left( \frac{N_3}{N_1^2} \right) i_3 + \left( \frac{N_4}{N_1^2} \right) i_4 \right]\tag{34}$$

$$L_{1m} = \frac{N_1^2}{\mathfrak{R}_c}\tag{35}$$

where,  $\mathfrak{R}_c$  is the reluctance of the magnetic core path and  $L_{1m}$  is the magnetizing inductance of the primary winding.

By converting the Equations (26) through (29) in the form of the state equation, we have:

$$\begin{bmatrix} \bullet \\ x_1 \\ \bullet \\ x_2 \\ \bullet \\ x_3 \\ \bullet \\ x_4 \end{bmatrix} = \begin{bmatrix} a_{11} & a_{12} & a_{13} & a_{14} \\ a_{21} & a_{22} & a_{23} & a_{24} \\ a_{31} & a_{32} & a_{33} & a_{34} \\ a_{41} & a_{42} & a_{43} & a_{44} \end{bmatrix} \begin{bmatrix} x_1 \\ x_2 \\ x_3 \\ x_4 \end{bmatrix} + \begin{bmatrix} b_{11} \\ b_{21} \\ b_{31} \\ b_{41} \end{bmatrix} * U\tag{36}$$

$$y = [c_{11} \quad c_{12} \quad c_{13} \quad c_{14}] \begin{bmatrix} x_1 \\ x_2 \\ x_3 \\ x_4 \end{bmatrix}\tag{37}$$

where,  $U$  is identity matrix and the coefficients of the  $A$  and  $B$  matrixes are dependent to the windings characteristics: Internal resistance, self and mutual leakage inductance.

$$a_{ij} = f(l_{ij}, R_i, R_a, N_i), \quad i, j \in \{1, 2, 3, 4\}\tag{38}$$

$$b_{ij} = g(l_{ij}, R_i, R_a, N_i), \quad i, j \in \{1, 2, 3, 4\}\tag{39}$$

$$c_{ij} \in \{0, 1\}\tag{40}$$

Each of the coefficients with respect to boundary condition was simply obtained from (26) through (29).

The optimum performance of the active shielding coils adoption in an electromagnetic system based on the above mentioned criterions

for system stability was clarified by solving the state equation corresponding to Equation (30) for the following cases:

Case 1: For  $x_4 = 0$  and  $x_4 \neq 0$ , the results show that the system is more stable when  $x_4 \neq 0$  that is, the roots are closer to the origin  $(0, 0)$ .

Case 2: The values of  $R_a = 0$  and  $R_a > 0$  were substituted in  $a_{ij}$  and  $b_{ij}$  coefficients. The results showed that for  $R_a = 0$  the roots are nearer to the origin.

As a consequence, for the proposed active shielding circuit, the compensating current  $i_{\text{aux}}$  must flow through  $N_3$  and  $N_4$ , with the lowest connection resistance value in the circuit.

## 5. CASE STUDY: CIT PARAMETERS

To estimate the effect of the compensating coils on leakage field mitigation, the proposed method was implemented on a 25 kA single phase CIT. Initially the leakage field distribution in the CIT in the presence and absence of compensating coils was calculated through computer simulation using FEM [13, 14].

The generalized expressions for the active shielding developed in the present paper are new. Since the computations are simple and straightforward with the help of **FEM** mathematical analysis [14], even though lengthy, we shall only quote and analyze the results for various interesting cases.

As it was mentioned earlier, a 125 kVA–25 kA single-phase CIT was designed and simulated to investigate the new approach [13]. The most important design parameters of the CIT are shown in Table 1.

### 5.1. Simulation of Magnetic Leakage Fields in the CIT System

The FEM of an electromagnetic system is performed in order to verify the effectiveness of the theoretical equations used in the design process and validate the designed parameters [13, 15, 16]. Automatic mesh generation and adaptivity for FEM plays an important role in electromagnetic systems. The optimal mesh density was generated automatically by the system according to the boundary curvature, thickness element number, the field variable gradient distribution of temperature, strain and strain rate, and density window [17–20].

In this paper, the mesh generation, based on adaptive meshing method, the generation/changing of a mesh and finite element analysis were repetitively performed, and during these repetitions, the mesh was dynamically changed in accordance with the analysis results.

**Table 1.** Design parameters of the studied transformer with compensating winding.

Rating	Capacity Voltage Current Frequency Phase	125 kVA 400/5 V 312.5/25000 A 50 Hz Single-phase
Core	Max. Field Density Cross Section Area Materials	1.6 T 140.6 cm <sup>2</sup> 30 M5
Main Windings	Material Conductor Cross Section No. of Primary Parallel Conductors No. of Secondary Parallel Conductors $J_c$ V/T	Copper 11 × 1.9 mm <sup>2</sup> 2 160 7.585 A/mm <sup>2</sup> 5 V
Compensating Winding	Material $J_c$ No. of Turns	Copper 5.7 A/mm <sup>2</sup> 30

In the calculation of flux, the main flux and leakage flux paths were identified [13, 21]. The values of the reluctance and permeance were assigned. The main flux follows the magnetic core paths and links the main coils of the primary and secondary windings. The variations of field distribution within the CIT windows for both cases: Without and with compensating coils are shown in Figs. 5 and 6 respectively. However, it will be appreciated by those skilled in the art that, the condition required for an adequate analysis of a mesh differ between Figs. 5 and 6, depending on the analysis type for without and with auxiliary winding conditions. As such, to increase the analysis accuracy, it was preferable that a smaller mesh be used at and around the periphery of the window of the CIT with compensating coils (Fig. 6). However, the difference of the identical mesh generation in Figs 5 and 6, is below 1%.

It is evident that the maximum axial component of the flux density  $B_y$  (red colour plot) occurs along the centre of the coil. Although,

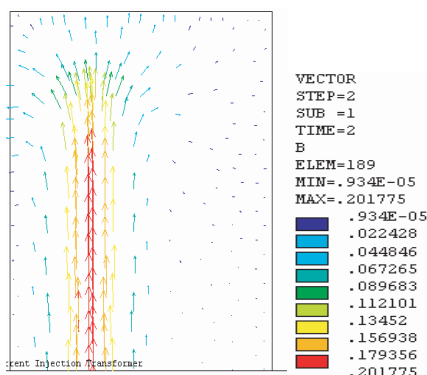


**Figure 5.** Magnetic field distribution in the window of the CIT without compensating coils.

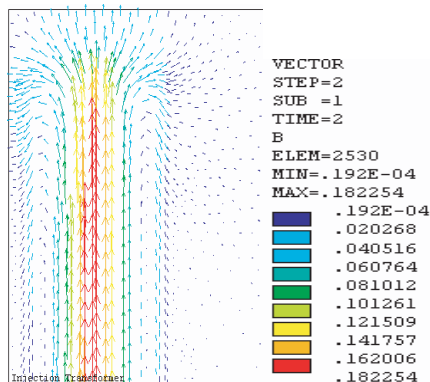


**Figure 6.** Magnetic field distribution in the window of the CIT with compensating coils (for  $R_a = 0$ ).

Fig. 5 can be verified by Equation (41) [16].

$$B_y = \mu_0 \frac{\sqrt{2}IN}{\ell} \tag{41}$$

where,  $IN$  is the ampere-turns of the coil and  $\ell$  is the coil length.

The flux density at any point of the CIT is found from this color plot. It can be noticed from the plot shown in Fig. 5 that the maximum of leakage magnetic flux density is 0.201787(T) while in Fig. 6 is reduced to 0.182265(T). As such, field reduction of 9.67% for maximum leakage fields is achieved. However, as stated in Section 1, the fields escape the core and windings of the transformer can bring about disturbing electromagnetic environment which may lead to electromagnetic interferences (EMI) with other neighboring sensitive components/systems. In this case, the effective solution is passive shielding of the victim component/system. Although the minimum values of the leakage magnetic fields, in this study, are increased (around  $\mu\text{T}$ ), this will have no effects on EMC or practical considerations (i.e., mechanical and thermal stresses) and should not be considered as possible EMI source.

### 5.2. Verification of Simulation Results Using State Equation

According to state Equations (33) through (40), calculation of eigenvalues for the CIT system confirms the simulation results. The CIT system poles and the dominant pole for various cases are

shown in Table 2. Moreover, this theory proves that the connection configuration of the compensating coils is valid. By comparing the dominant poles with each other, it is found that the most dominant pole is the one being located in the left half plane close to the origin and to be 5 to 10 times greater than the others. Having considered that, for this study in Table 2, the highest rank of the dominant pole belongs to the case with compensating windings when  $R_a = 0$  and then for the cases  $R_a = 20 \Omega$  and  $R_a = 50 \Omega$ , respectively. However, it can be deduced that the short circuited compensating coils is the most suitable case for the leakage field shielding purposes.

Furthermore, to clarify the implications of “fast convergence” for optimal shielding, such an approach can be achieved when the roots are close to the origin where, faster compensation takes place.

FEM simulations have also been performed for  $R_a = 20 \Omega$  and  $R_a = 50 \Omega$ , which are used to verify the mathematical results shown in Table 2, and the corresponding maximum leakage flux density values shown in Table 3. It is clearly evident that, simulation results in Table 3 show good correspondence with Table 2.

In addition, performance of the CIT may be affected easily by the leakage flux. Because, for 25 kA output current the maximum admissible impedance is  $200 \mu\Omega$ . This implies that the leakage reactance must be minimal. Moreover, leakage flux will have detrimental effect of mechanical force on the CIT windings.

**Table 2.** Computation of system poles for various states.

Cases	System poles	Dominant pole
without compensating windings	$s_1 = -1.9313 \times 10^8$ $s_{2,3} = (-0.000029 \pm 0.000861j) \times 10^4$	$s_2 = (-0.000029 - 0.000861j) \times 10^4$
with compensating windings, for $R_a = 0$	$s_1 = -6.9522 \times 10^4$ $s_2 = -0.0014 \times 10^4$ $s_{3,4} = (-0.1439 \pm 8.9159j) \times 10^4$	$s_2 = -0.0014 \times 10^4$
with compensating windings, for $R_a = 20 \Omega$	$s_1 = -0.0121 \times 10^6$ $s_2 = -6.7036 \times 10^6$ $s_{3,4} = (-0.0018 \pm 0.0437j) \times 10^6$	$s_3 = (-0.0018 - 0.0437j) \times 10^6$
with compensating windings, for $R_a = 50 \Omega$	$s_1 = -0.02765$ $s_2 = -3.2371 \times 10^6$ $s_{3,4} = (-0.0024 \pm 0.0543j) \times 10^6$	$s_3 = (-0.0024 - 0.0543j) \times 10^6$

**Table 3.** FEM results of leakage flux density for various states.

Cases	$B_{max}$ (T)	field improvement
without compensating windings	0.201775	-
with compensating windings, for $R_a = 0$	0.182265	9.67%
with compensating windings, for $R_a = 20$	0.187743	6.95%
with compensating windings, for $R_a = 50$	0.188459	6.60%

### 5.3. Mechanical Force Improvement

It is well known that, mechanical stress can have harmful effects on the system in which one trend stood out and warrants special attention — The issue of the CIT age [22, 23]. The electromagnetic forces that act at the transformer windings are generated by the interaction between current density and leakage field density. These forces can be calculated using (42):

$$\vec{F} = \vec{J} \times \vec{B} \tag{42}$$

where:  $\vec{F}$  is the force density vector,  $\vec{J}$  is the current density vector and  $\vec{B}$  is the leakage flux density vector.

It is important to note that the magnetic flux density is also a function of current; therefore, calculations of force will always be

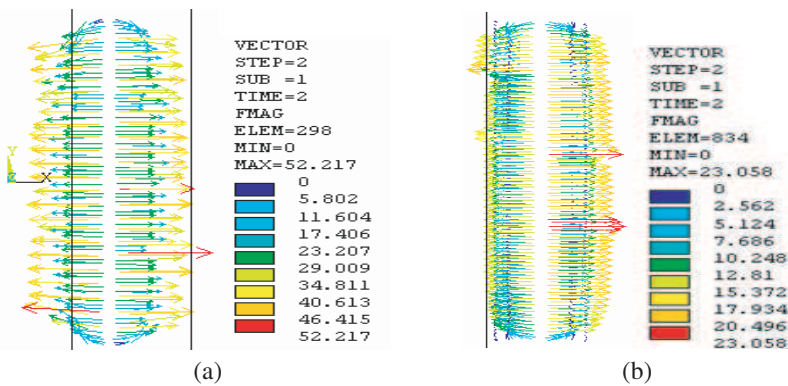


**Figure 7.** Distribution of electromagnetic force density in the window of the CIT. (a) Without and (b) with compensating windings.

proportional to the product of the current squared. Proportional to the current squared, mechanical forces increase rapidly.

Referring to Figs. 7(a) and (b), the simulated localized force density distributions show good correspondence to the localized flux density distributions shown in Figs. 6(a) and (b). The force density simulation results in Figs. 7(a) and (b), show an improvement of 55.84% by compensating coil arrangement.

## 6. CONCLUSION

This paper presented a new method of winding arrangements so as to reduce the leakage magnetic field by adapting an active shielding to generate a counter field opposite to the leakage fields leaking from an iron-core system. This strategy mitigates the leakage fields and consequently reducing mechanical forces due to high current. The simulation results were confirmed with the mathematical model based on the theory of electromagnetic coupled circuits.

The leakage fields were calculated in the presence and absence of compensating windings by FEM analysis and the corresponding results were validated with the proposed mathematical proofs of the concept. The mathematical proofs based on related dominant poles of the active shielding to be as close to the origin as possible, using state equations. As such, fast convergence of the solutions was studied and optimal CIT performance was achieved.

As a case study, compensating windings performances were simulated by FEM analysis in a 125 kVA, 25 kA CIT system. The results showed an improvement of leakage fields and thereby reducing the corresponding mechanical forces.

The present approach contemplates an arrangement for reducing leakage flux and consequently mechanical forces. However, it will be readily apparent to those skilled in the art that it is possible to embody the phenomena in specific electromagnetic systems other than that described above without departing from the spirit of the concept.

## REFERENCES

1. Robertson, J.-B., E. (T.) A. Parker, B. Sanz-Izquierdo, and J. C. Batchelor, "Electromagnetic coupling through arbitrary apertures in parallel conducting planes," *Progress In Electromagnetics Research B*, Vol. 8, 29–42, 2008.
2. Koontz, R., M. Akemoto, S. Gold, A. Kransnykh, and Z. Wilson, "NLC klystron pulse modulator R&D at SLAC," *Proceedings IEEE Conference on Magnetics*, 1319–1321, 1998.

3. Li, J., Z. Wang, Y. Wang, M. Gao, and H. Wang, "Effect of mutual inductance on the pulsed current amplification of magnetic field compressors," *IEEE Transactions on Magnetics*, Vol. 37, No. 1, 489–492, 2001.
4. Heydari, H., S. M. Pedramrazi, and F. Faghihi, "The effects of windings current density values on leakage reactance in a 25 kA current injection transformer," *IEEE Conference, IPEC*, 2005.
5. Buccella, C., M. Feliziani, and A. Prudenzi, "Active shielding design for MV/LV distribution substation," *3rd International Symposium on Electromagnetic Compatibility*, 350–353, 2002.
6. Fang, C.-H., S. Zheng, H. Tan, D. Xie, and Q. Zhang, "Shielding effectiveness measurements on enclosures with various apertures by both mode-tuned reverberation chamber and gtem cell methodologies," *Progress In Electromagnetics Research B*, Vol. 2, 103–114, 2008.
7. Bahadorzadeh, M., M. Naser-Moghadasi, and A. R. Attari, "Improving of shielding effectiveness of a rectangular metallic enclosure with aperture by using extra wall," *Progress In Electromagnetics Research Letters*, Vol. 1, 45–50, 2008.
8. Lei, J.-Z., C. H. Liang, and Y. Zhang, "Study on shielding effectiveness of metallic cavities with apertures by combining parallel FDTD method with windowing technique," *Progress In Electromagnetics Research*, PIER 74, 85–112, 2007.
9. Faghihi, F. and H. Heydari, "Time domain physical optics for the higher-order FDTD modeling in electromagnetic scattering from 3-D complex and combined multiple materials objects," *Progress In Electromagnetics Research*, PIER 95, 87–102, 2009.
10. Lipschutz, S. and M. Lipson, *Linear Algebra*, 3rd edition, Schaum's Outlines, 2000.
11. Chen, B. M., Z. Lin, and Y. Shamash, *Linear System Theory*, Birkhauser, 2004.
12. Heydari, H. and F. Faghihi, "Hybrid winding configuration in high current injection transformers based on EMC issues," *IET Electr. Power Appl.*, Vol. 3, No. 3, 187–196, 2009.
13. Heydari, H., M. Ariannejad, and F. Faghihi, "Simulation and analysis of 25 kA current injection transformer (CIT) with finite element method," *IEEE Conference, Melecon*, 909–915, 2004.
14. Faghihi, F., H. Heydari, A. Falahati, and Y. A. Easy, "Convolutional codes acting as EMI virtual shields in current injection systems," *Progress In Electromagnetics Research*, PIER 88, 337–353, 2008.

15. Bedrosian, G., "High-performance computing for finite element methods in low-frequency electromagnetics," *Progress In Electromagnetics Research*, PIER 07, 57–110, 1993.
16. Baldwin, L. T., I. J. Ykema, L. C. Allen, and L. J. Langston, "Design optimization of high-temperature superconducting power transformers," *IEEE Transactions on Applied Superconductivity*, Vol. 13, No. 2, 2344–2347, 2003.
17. Zhang, P.-F., S.-X. Gong, and S. F. Zhao, "Fast hybrid FEM/CRE-UTD method to compute the radiation pattern of antennas on large carriers," *Progress In Electromagnetics Research*, PIER 89, 75–84, 2009.
18. Wang, Q. and X.-W. Shi, "A an improved algorithm for matrix bandwidth and profile reduction in finite element analysis," *Progress In Electromagnetics Research Letters*, Vol. 9, 29–38, 2009.
19. Tai, C.-C. and Y.-L. Pan, "Finite element method simulation of photoinductive imaging for cracks," *Progress In Electromagnetics Research Letters*, Vol. 2, 53–61, 2008.
20. Vaish, A. and H. Parthasarathy, "Analysis of a rectangular waveguide using finite element method," *Progress In Electromagnetics Research C*, Vol. 2, 117–125, 2008.
21. Hatamzadeh-Varmazyar, S. and M. Naser-Moghadasi, "New numerical method for determining the scattered electromagnetic fields from thin wires," *Progress In Electromagnetics Research B*, Vol. 3, 207–218, 2008.
22. Shiri, A. and A. Shoulaie, "A new methodology for magnetic force calculations between planar spiral coils," *Progress In Electromagnetics Research*, PIER 95, 39–57, 2009.
23. Formato, R. A., "Central force optimization: A new metaheuristic with applications in applied electromagnetics," *Progress In Electromagnetics Research*, PIER 77, 425–491, 2007.